Sea ice melt drives vertical pCO_2 variability modulating air-sea gas exchange

Henry C. Henson[1,2], Dorte H. Søgaard[2,3,7], Bjarne Jensen[6], Kunuk Lennert[4], Tim Papakyriakou[5], Mikael K. Sejr[1,2], Jakob Sievers[6], Søren Rysgaard[2,7], and Lise Lotte Sørensen[2,6]

[1]Department of Ecoscience, Aarhus University, Aarhus, 8000, Denmark
[2]Arctic Research Center, Aarhus University, Aarhus, 8000, Denmark
[3]Greenland Climate Research Cluster, Greenland Institute of Natural Resources, Nuuk, 3900, Greenland
[4]UiT, The Arctic University of Norway, Tromsø, 9037, Norway
[5]Centre for Earth Observation Science, University of Manitoba, Winnipeg, MB, R3T 2N2, Canada
[6]Department of Environmental science, Aarhus University, Roskilde, 4000, Denmark
[7]Department of Biology, Center for Ice-free Arctic Research, Aarhus University, Aarhus, 8000, Denmark

Corresponding author: Henry C. Henson (hch@ecos.au.dk)

Key Points:

- Spring melting of sea ice and snow introduces distinct heterogeneity in surface water conditions within coastal Arctic oceans.
- Standard bulk parameterizations for air-sea CO_2 flux calculations, based on subsurface pCO_2 measurements, may misrepresent flux ~~direction and~~ magnitude during melt periods.
- Vertical near-surface ~~temperature and~~ CO_2 and temperature gradients must be considered to improve flux estimates in stratified Arctic fjords.

Abstract

Strong spatial and temporal gradients in salinity, temperature, and carbonate chemistry in Arctic coastal surface waters complicate the estimation of air-sea carbon dioxide (CO_2) exchange, particularly during sea ice breakup. ~~Our~~ The present study evaluates the applicability of the widely used bulk flux model under such conditions. This approach assumes homogeneous surface conditions and no vertical pCO_2 gradients in the bulk seawater. However, our observations in a stratified Arctic fjord reveal pronounced vertical variability in pCO_2 within the upper water column, including non-linear gradients near the air-sea interface. This results in, widely varying flux estimates depending upon the depth of the pCO_2 measurement used to establish air-sea disequilibrium. ~~Micrometeorological flux estimates suggested variability in the direction of gas transfer, even when waters at 1 m depth and below were CO_2-undersaturated. We hypothesize that transient, high-pCO_2 layers within the upper decimeters intermittently decouple the atmospheric exchange from subsurface waters and have the potential to reverse the expected flux direction.~~ These findings highlight the importance of resolving near-surface variability during the transition from ice-covered to open water conditions. We recommend incorporating both micrometeorological techniques and high-resolution vertical profiling in Arctic fjords to improve flux estimates of CO_2 in this rapidly changing region.

Plain Language Summary

Sea ice melt adds less-saline water to the surface ocean. This creates vertical gradients in salinity, temperature, and partial pressures of carbon dioxide (pCO_2). The concentration difference of pCO_2 across the air-ocean boundary is used to estimate gas transfer. Thus, the depth that we measure will impact our estimates. ~~Directly measuring gas transfer showed both CO_2 uptake and release from the ocean during sea ice breakup.~~ This means ocean layering during ice melt may slow or briefly reverse the direction of CO_2 transfer.

1 Introduction

High latitude coastal oceans are strong sinks for atmospheric carbon dioxide (CO_2), absorbing more CO_2 per unit area than lower latitude regions (Dai et al., 2022; Roobaert et al., 2019). This strong uptake results from both the high solubility of gases in cold water and the intense biological activity typical of these regions. However, climate change is rapidly transforming this carbon sink. The Arctic is warming more than twice as fast as the global average, and sea ice extent has been shrinking by over 13% per decade (Perovich et al., 2020). The loss of sea ice increases CO_2 uptake by exposing larger areas of open water for longer periods, which can further stimulate biological productivity (Arrigo and van Dijken, 2015; Bates and Mathis, 2009; Perovich et al., 2020). However, at the same time, melting sea ice freshens the surface layer and strengthens stratification, limiting vertical mixing with deeper water. Freshwater from melting sea ice and terrestrial run-off creates pronounced gradients in physical properties such as salinity and temperature, as well as chemical properties like dissolved inorganic carbon (DIC) and total alkalinity (TA) (e.g. Henson et al., 2025). As a result, the partial pressure of CO_2 (pCO_2) can

vary markedly with depth under melt conditions (Miller et al., 2019).

This vertical variability in pCO_2 poses a challenge for air-sea CO_2 flux estimation. The transfer of gases between the atmosphere and ocean depends on the difference in concentration between the two as well as the efficiency of the transfer process. Therefore, the bulk flux of CO_2 across the air-sea interface is commonly described as the product of the gas transfer velocity, k (m s^{-1}), CO_2 solubility s (mol kg^{-1} atm^{-1}), and the partial pressure gradient (µatm) across the air-sea interface (Wanninkhof et al., 2009):

$$F = ks(pCO_{2_{sea}} - pCO_{2_{air}}) \quad (1)$$

While widely applied, this formulation simplifies a complex process influenced by surfactants on the water surface, bubble-mediated gas exchange, and turbulence (Wanninkhof et al., 2009). Furthermore, surface water heterogeneity, driven by sea ice melt and freshwater runoff from land, complicate the physical and chemical processes governing air-sea CO_2 exchange. As a result, simplified parameterizations commonly used in global carbon flux estimates may be inadequate in these settings.

In most studies, pCO_2 is measured several meters below the surface, assuming vertical homogeneity under well-mixed condition (Jørgensen et al., 2020). However, in stratified waters, where temperature, salinity, and pH can vary with depth, this assumption may lead to substantial errors in flux estimates (Ahmed et al., 2020; Dong et al., 2021; Miller et al., 2019; Watts et al., 2022). Although Arctic surface waters are often undersaturated with respect to atmospheric CO_2 levels and act as CO_2 sinks (e.g., Burgers et al., 2017; Dai et al., 2022; Henson et al., 2024; Laruelle et al., 2014; Roobaert et al., 2019), such assessments typically rely on sparse data collected from 0.5-5 m depth during limited periods. Dong et al. (2021) illustrate that high latitude fluxes of CO_2 calculated using the bulk method (based on measurements sampled at 6 m depth) differ significantly from those measured using direct eddy covariance in sea ice melt regions.

Gas transfer velocity (k) is often parameterized as a function of wind speed. However, the true driver is mixing in the surface waters, which governs k. Fick's first law of diffusion, which underlies Equation (1), assumes a linear concentration gradient within the diffusive sublayer (Fig. 1) and steady-state conditions (Garbe et al., 2014). Jørgensen et al. (2020) argued that, due to seawater's high buffer capacity, chemical gradients do not significantly affect CO_2 equilibration, supporting the use of measurements at 3-4 m depth. However, this conclusion relies on the assumption of horizontal and vertical homogeneity and neglects the effects of shallow surface stratification, particularly when alkalinity dilution is involved.

In Arctic spring, the upper ocean is often strongly stratified due to freshwater input from glacier melt, snowmelt, river runoff, and sea ice meltwater (Ahmed et al., 2020; Granskog et al., 2011; Meire et al., 2017; Miller et al., 2019). These inputs can extend vertical CO_2 gradients beyond the diffusive sublayer, complicating flux estimates during ice break-up and early open-water periods. Several studies have demonstrated strong vertical heterogeneity in pCO_2 in Arctic coastal waters, with implications for air-sea flux calculations (Ahmed et al., 2020; Dong et al., 2021; Miller et al., 2019).

Surface freshening from ice melt and runoff strongly influences carbonate chemistry in Arctic coastal waters, which can either suppress or enhance oceanic CO_2 uptake. For example, Burgers et al. (2017) reported large horizontal variability in surface pCO_2 (144–364 µatm) linked to riverine input in the Eastern Canadian Arctic. Similarly, Sejr et al. (2011) observed strong surface pCO_2 gradients associated with salinity and temperature in Young Sound, and later documented a long-term decline in surface salinity (Sejr et al., 2017). Freshwater-induced stratification has also been shown to create vertical gradients in pCO_2 and pH with important implications for flux calculations (Miller et al., 2019). Finally, Bates et al. (2014) demonstrated that sea ice meltwater and melt ponds exhibit extreme variability in pCO_2 (<10 to >1500 µatm) and pH (6.1 to >10.8), highlighting the complex chemical landscape of ice-influenced waters. Together, these studies underscore the high spatial and temporal variability of carbonate chemistry in freshened waters across the Arctic.

To project future CO_2 uptake or outgassing in the Arctic, we must better understand the physical and chemical drivers of near-surface carbonate variability. In this study, we investigate the vertical and temporal variations in pCO_2 in a stratified Arctic fjord during sea ice breakup. By ~~combining~~ examining water-column pCO_2 profiles ~~with micrometeorological flux measurements~~ across the transition from ice-covered to open water, we evaluate ~~the applicability~~usage of the bulk flux model under Arctic seasonal transitions.

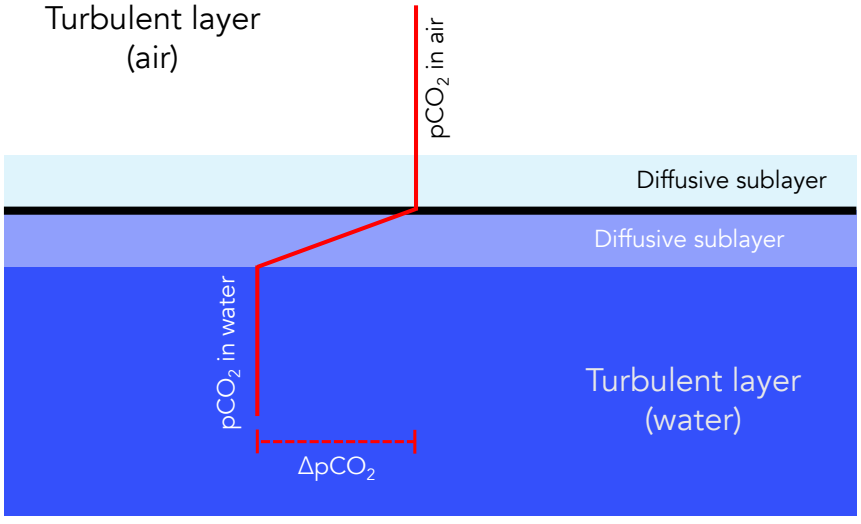

Figure 1. Schematic illustrating the interface between the air and the water in conjunction with pCO_2 concentration gradients. In equation 1, the concentration gradient is assumed to occur in the diffusive layer between the air and water, and the concentrations are assumed to be vertically constant in the turbulent layers. (Adapted from Liss and Slater, 1974; Wanninkhof et al., 2009)

2. Study Site and Measurement Methods

2.1 Study Site

This study was conducted in Young Sound, a high Arctic fjord system located near the Daneborg Research Station in Northeast Greenland (Fig. 2). The fjord system comprises the Tyrolerfjord (inner fjord) and Young Sound (outer fjord), extending approximately 90 km from Tyroler River to the Greenland Sea. A sill at about 45 m depth separates Young Sound from the open ocean. Young Sound is 2 to 7 km wide, with an average depth of 100 m (maximum 350 m), and a total surface area of ~390 km^2. Tidal amplitudes range from 0.8 to 1.5 m, with mean current velocities of approximately 2 cm s^{-1} (Rysgaard et al., 2003). Freshwater inputs are primarily derived from Greenland Ice Sheet runoff, local glaciers, precipitation, and snowmelt from adjacent ice-free terrain. The drainage basin of the Tyrolerfjord/Young Sound system spans 2846 km^2, of which 33% is glaciated.

Sampling was conducted from 12 to 31 July 2017. Sampling occurred during and immediately after a period of sea ice breakup. On 15 July, ice coverage was approximately 30%, decreasing to less than 10% by 16 July. Water sampling was conducted both from an inflatable boat and via sea ice leads, all in close proximity to the Greenland Ecosystem Monitoring (GEM) program's standard station (Fig. 2).

2.2 pCO_2 Measurements Using the HydroC Sensor

Surface water pCO_2 was measured with a CONTROS® HydroC CO_2 sensor, which utilizes a membrane equilibrator coupled with a non-dispersive infrared detector. The instrument is equipped with a built-in water pump that provides flow rate of 35 ml s^{-1} across the membrane. At each sampling depth, the sensor was allowed to equilibrate for 10 to 20 minutes, and values were recorded once stable for at least two minutes. The sensor operates over a range of 200-1000 µatm and temperatures of -2 to 35°C. Annual calibration has been conducted using a certified 400 ± 2% ppm CO_2 gas that was traceable to WMO standards. The sensor showed remarkable stability (397-401 ppm), supporting a measurement uncertainty of ± 2 µatm.

2.3 pCO_2 Estimation from TA and DIC

In addition to direct measurements, pCO_2 was calculated from total alkalinity (TA) and dissolved inorganic carbon (DIC) using the Seacarb package (Gattuso et al., 2024) in R. Due to the low salinity and cold temperatures characteristic of Arctic coastal waters, no universally accepted set of equilibrium constants (K1 and K2) exists. For consistency with previous studies in the region (Henson et al., 2023), we used the refitted constants from (Lueker et al., 2000). The selection of

equilibrium constants introduces assumptions regarding seawater composition. (Raimondi et al., 2019) showed that different constants can lead to discrepancies between measured and calculated pCO_2 values, ranging from -3.1 to -35.8 µatm, with Lueker et al. (2000) demonstrating the best internal consistency under polar conditions. Still, (Sulpis et al., 2020) found that the calculation of pCO_2 from DIC and TA can lead to uncertainty up to 15% under cold conditions, which is far greater than when pCO_2 is measured directly.

2.4 Sea Ice TA and DIC Sampling

TA and DIC in sea ice were assessed using three ice cores. Each core was sectioned into 5-10 cm segments and sealed in gas-tight NEN/PE bags with sampling valves (Hansen et al., 2000). Samples were transported in thermally insulated boxes to a nearby field laboratory. Cold (1°C) deionized water of known mass and carbonate composition (10 - 30 ml) was added to each bag, which was then resealed after removing air and weighted.

The samples were melted in the dark over ~48 hours. Meltwater was transferred to 12 mL Exetainer vials (Labco, UK) pre-dosed with 20 µl of saturated $HgCl_2$ solution (5% w/v) to prevent microbial alteration. DIC was measured by on Apollo SciTech®'s AS-C3 analyzer while TA was determined via potentiometric titration on an Apollo SciTech AS-ALK2 total alkalinity titrator (Haraldsson et al., 1997).

2.5 Physical Parameters

Vertical profiles of conductivity, temperature, and depth (CTD) were obtained using a Seabird® SBE19plus CTD. On 16 July 2017, additional surface conductivity measurements were taken using a Thermo Orion-Star® instrument with an Orion 013610MD conductivity cell. Surface water temperatures were independently measured with a Testo® thermometer.

2.6 Historical Data

For contextual comparison, pCO_2 time series data from the Greenland Ecosystem Monitoring program are also included in the analysis. pCO_2 data from 2007-2023 was measured using the same HydroC CO_2 sensor in August each year.

2.7 Eddy Covariance

~~Air-sea CO_2 fluxes, as well as s~~Sensible and latent heat fluxes~~,~~ were estimated using micrometeorological instrumentation mounted on a 3-meter mast positioned approximately 0.5 meters from the waterline. ~~CO_2 concentrations were measured with a LI-COR® 7500 open-path gas analyzer, and t~~Three-dimensional wind vectors were recorded using a METEK® uSonic-Scientific sonic anemometer. ~~The open-path analyzer was used at the time due to its low power consumption, suitable for operation on battery systems in remote Arctic environments. However, the authors recognize that open-path sensors over polar, marine environments can lead to larger errors due to the cross-sensitivity between humidity and CO_2 for near infrared gas~~

~~analyzers (Blomquist et al., 2014; Landwehr et al., 2014). As a result, we do not aim to precisely constrain CO_2 flux magnitudes throughout the study but provide support for the profiles measured throughout this seasonal transition.~~

To enhance reliability, we applied complementary analysis techniques for flux estimation: (1) the standard eddy covariance (EC) method using EddyPro software (Version 7.0.6, LI-COR Inc., 2019); (2) the ogive optimization method (OGM) (Sievers et al., 2015a). Among these, the OGM was deemed most robust due to its ability identify and filter out low-frequency noise, sensor dampening, and large-scale turbulent motions that can bias flux measurements. These issues often introduce large relative bias associated with flux measurement over ~~surfaces characteristically exhibiting low CO_2 fluxes, such as~~Arctic marine surfaces (Sievers et al., 2015b). OGM's superior ability to isolate relevant turbulent scales and reduce contamination from mesoscale variability is based on the accumulation and modelling of each cospectra over each 20 min averaging period (Fig. S1 and S2). Uncertainty in ~~CO_2~~ sensible and latent heat fluxes was estimated directly from the OGM procedure. The reported values correspond to the standard error associated with the fitted ogive tail and reflect random uncertainty in flux integration.

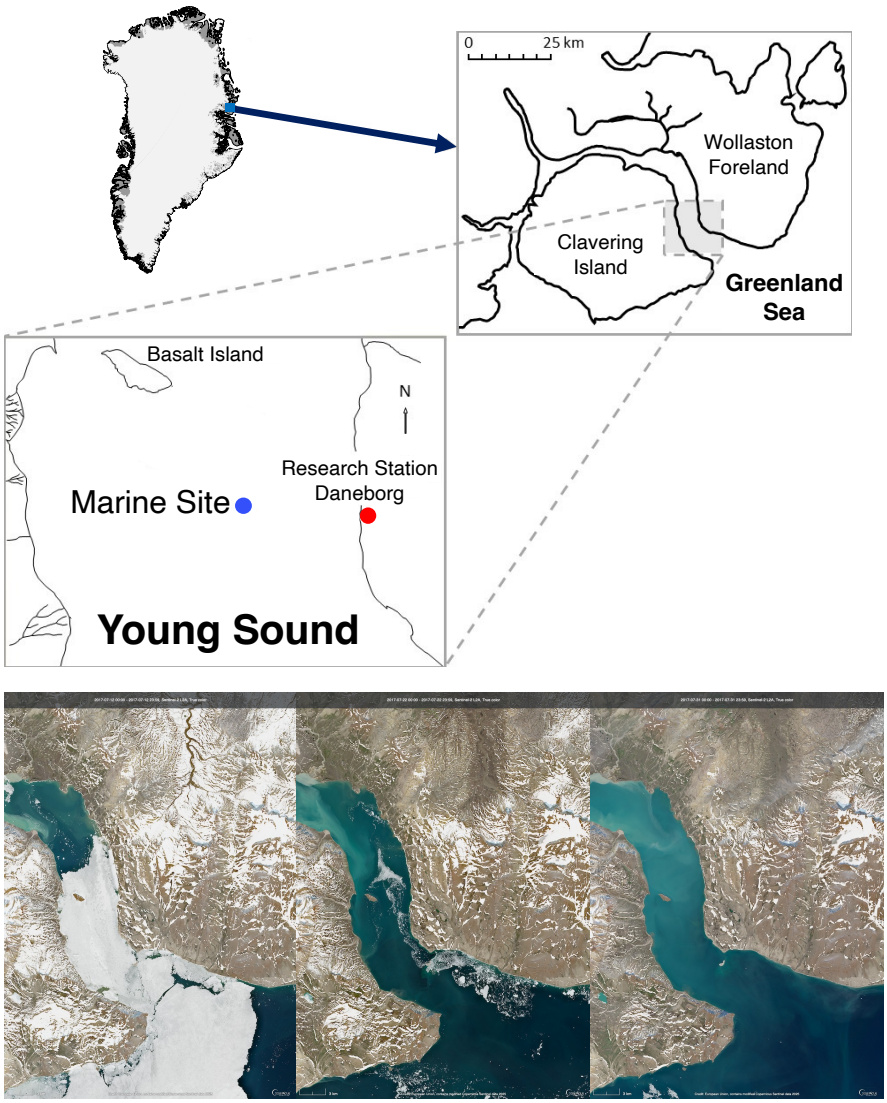

Figure 2. Map of Greenland and the sampling area at the coast of Young Sound in Northeast Greenland. The red circle indicates the location of the ~~Eddy Covariance tower~~ micrometeorological measurement tower at research station Daneborg while the m~~M~~arine sampling site (Standard Station in the Greenland Ecosystem Monitoring program) is indicated as a blue circle (74.310, -20.300). Three Copernicus Sentinel true-color images of the fjord on July 12, 22, and 31 illustrate the transition between sea ice cover and open water.

3 Data and results

~~3.1 CO_2 and Heat Fluxes~~

~~Surface air-sea CO_2 fluxes were measured using micrometeorological techniques between July 16 and July 31, 2017 (Fig. 3a). However, only a limited number of flux estimates passed the quality control criteria defined by OGM. This method uses a Haar wavelet analysis to assess the~~

~~continuity of high-frequency CO_2 and vertical wind velocity signals, rejecting fluxes when either variable fails to meet spectral continuity thresholds. In addition to the automated filtering, manual inspection of the cospectra was performed to evaluate fluxes that were soft-flagged by the Haar analysis. Only fluxes that passed both stages of evaluation were retained for further analysis and are shown in Fig. 3a (Fig. S1).~~

~~Fluxes measured using eddy covariance (EC) were highly variable throughout the period of sea ice melt, exhibiting both upward and downward fluxes. Positive values indicate net efflux of CO_2 from the ocean to the atmosphere, implying temporary oversaturation of surface waters with respect to atmospheric CO_2. EC-based effluxes were observed during and shortly after the sea ice breakup period. These estimates contrast with prior studies in Young Sound, which describe the fjord as a net CO_2 sink throughout the year (Sejr et al., 2011). However, historic estimates are based on pCO_2 measurements from the month of August and taken at 1 m depth; not from vertical pCO_2 profiles that capture salinity gradients. Similar episodic outgassing events have been documented in other Arctic coastal systems under variable sea ice conditions, though particularly during or following sea ice melt (Butterworth et al., 2025; Else et al., 2011; Miller et al., 2011; Papakyriakou and Miller, 2011; Prytherch and Yelland, 2021; Sievers et al., 2015c).~~

~~In addition to CO_2 fluxes, eddy covariance measurements of sensible and latent heat fluxes were also quantified during the same period and are presented in Fig. 3b and 3c. For all scalar quantities, negative values represent downward fluxes directed toward the ocean surface. These heat flux data provide important context for interpreting variability in CO_2 exchange, as they reflect changes in atmospheric forcing and surface stratification. Corresponding meteorological variables, including wind speed and air temperature, are shown in Fig. 3d-f.~~

~~The flux uncertainties shown in Fig. S3 quantify random uncertainty from the OGM integration procedure, and illustrate CO_2 uncertainties were typically below 5 mmol m^{-2} d^{-1}. Low uncertainties during both uptake and efflux events demonstrated a good signal to noise ratio and provide support for the integration of fluxes during these variable conditions. The highest uncertainties that exceed 5 mmol m^{-2} d^{-1} corresponded to near-zero fluxes, where precise flux-estimation becomes more difficult. However, these calculated uncertainties do not account for potential systematic bias related to water vapor cross sensitivity, which must be evaluated through other metrics.~~

~~3.2 Surface Water pCO_2~~

Vertical profiles of surface water pCO_2 were measured using the CONTROS® HydroC CO_2 sensor across three distinct periods in July 2017 (Fig. 3~~5~~a-c). Each observational period corresponded to different sea ice conditions: before, during and after sea ice breakup (Fig. 2). These high-resolution profiles revealed substantial vertical variability within the upper 2 to 3

meters of the water column. Under ice-covered conditions, pCO_2 measurements were taken through an open melt pond. At this time, elevated CO_2 concentrations were observed at the very surface (0.1 m), followed by a sharp decrease to approximately 1 meter depth, coinciding with the ice-water interface. Below this depth, pCO_2 increased again, though remained well below atmospheric concentrations (Fig. 34a).

During the period of sea ice breakup, when ice coverage ranged from approximately 30% to 10%, the vertical distribution of pCO_2 exhibited a similar structure. Concentrations were highest near the surface, declined to a local minimum at 1 to 2 meters, and then stabilized below 3 meters (Fig. 34b). Following, the complete breakup of sea ice, pCO_2 showed a more gradual decrease from the surface down to about 3 meters, beneath which concentrations remained relatively constant (Fig. 34c). Across all three observational periods, a shallow surface layer approximately 5 m thick was identified, within which most of the pCO_2 variability occurred. Below this depth, pCO_2 remained relatively constant.

These vertical structures are consistent with strong physical stratification, likely driven by freshwater input from glacial melt and surface heating. Temperature and salinity profiles collected concurrently support the presence of sharp vertical gradients in the upper water column, with salinity ranging from 1.4 to 29.6 PSU and temperature from -0.4°C to 6.2°C. These physical profiles, shown in Fig. 45, confirm that vertical mixing was strongly suppressed during the observational period. The small tides present in Young Sound, combined with the continued input of freshwater from first sea ice and then glacial melt, lead to a fjord system with distinct surface stratification throughout the months of July and August.

Measurements from a different fjord in East Greenland on June 4, 2025, revealed strikingly similar vertical pCO_2 heterogeneity (Fig. 56). Elevated pCO_2 at 0.1 m decreased to a minimum around 1-1.5 m before increasing again and stabilizing near 3 m depth. Extreme stratification in the upper few meters caused pCO_2 levels in each profile to vary by more than 100 µatm between the surface and 1 m. This repeated observation of comparable vertical pCO_2 heterogeneity 8 years later and in a different fjord system suggest this is not an isolated phenomenon. Indeed, Arctic surface stratification during sea ice breakup induces chemical changes that may influence the way we estimate air-sea exchange of CO_2.

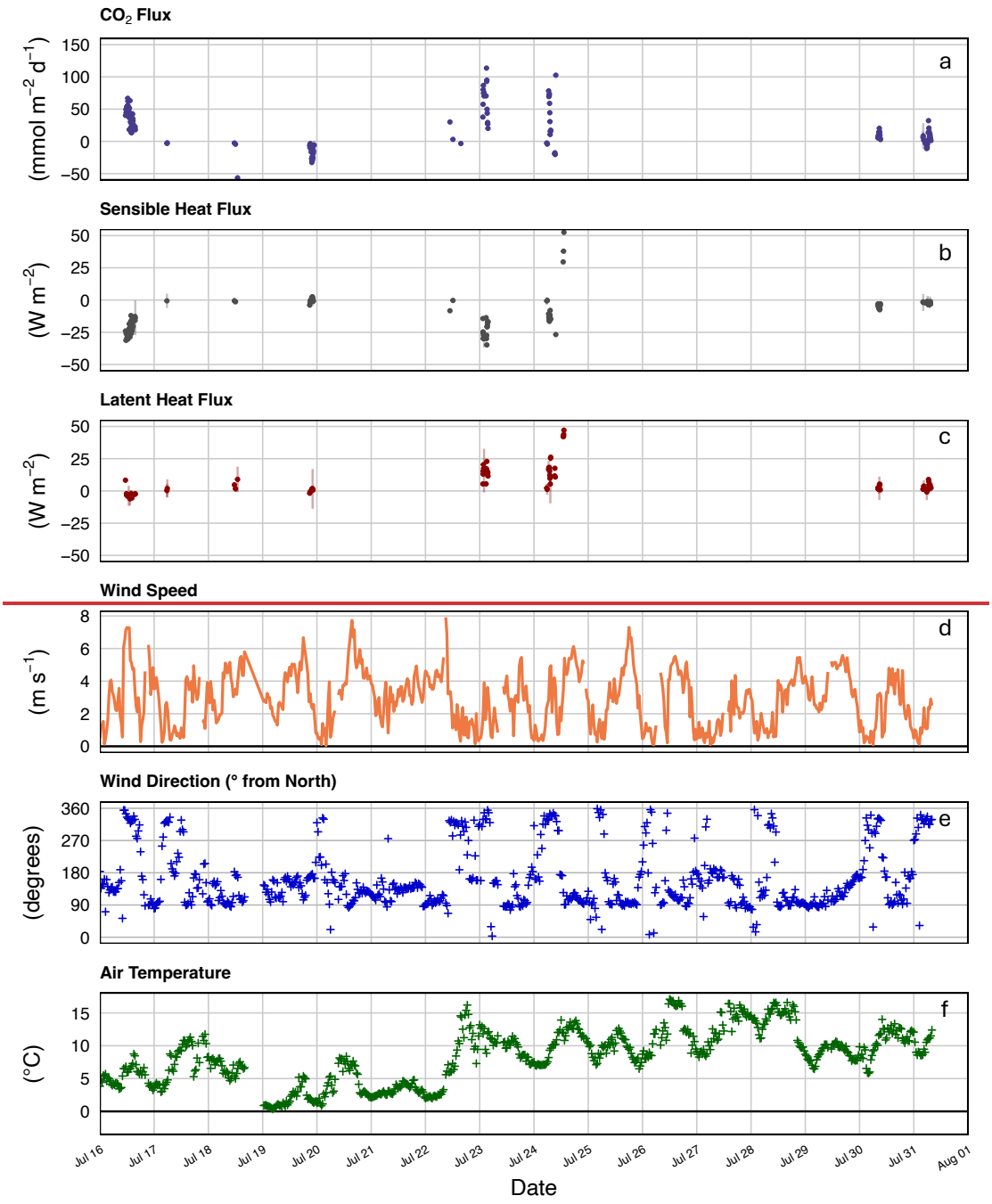

Figure 3. The 5 min averages of measured fluxes and meteorological conditions over Young Sound during July 2017. This time period reflects the transition between sea ice break up (30% ice cover) and open water (no sea ice present) from 16 July 2017 to 1 August 2017. Air-sea exchange of (a) CO_2 (b) sensible heat and (c) latent heat were estimated using the ogive optimization method with estimated uncertainty shown as vertical error bars. (d) Wind speed, (e) wind direction and (f) air temperature are shown for the same period. Note: Use of an undried air-stream in the open-path CO_2 sensor likely inflates the magnitude of the illustrated CO_2 fluxes due to water vapor cross sensitivity.

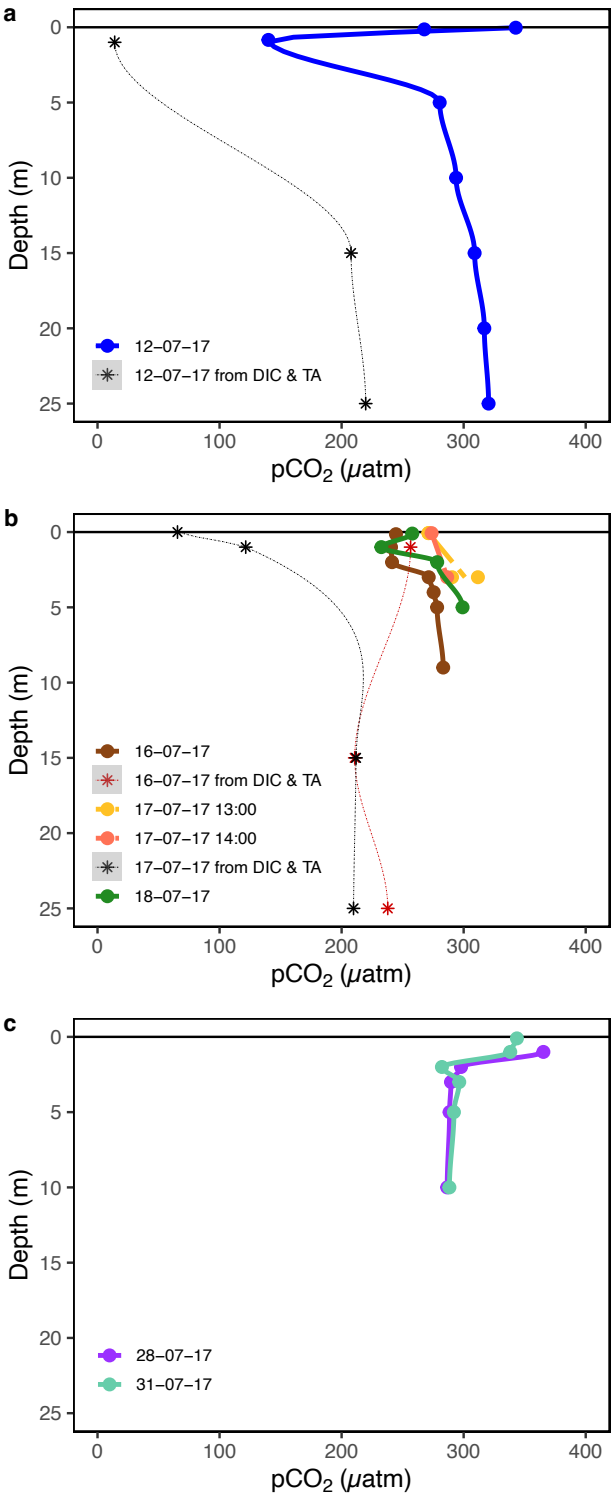

Figure 34. Measured Young Sound pCO_2 profiles (a) prior to sea ice breakup (measured through open melt pond), (b) during sea ice breakup and (c) after sea ice break up measured through CO_2 equilibration and calculation from carbonate chemistry parameters (DIC & TA).

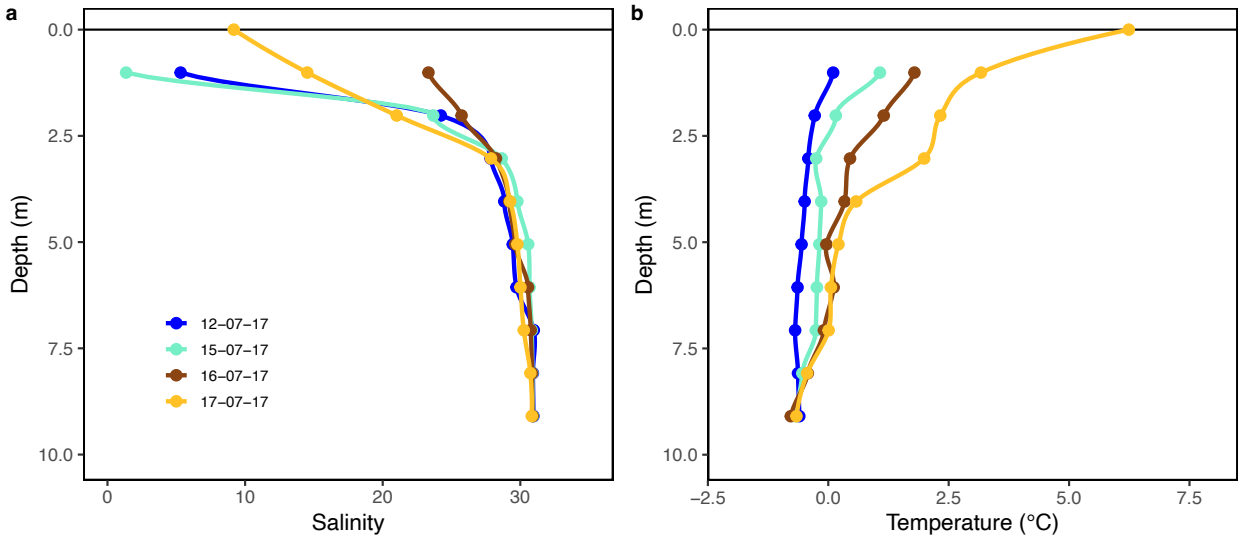

Figure 45. Measured Young Sound profiles of under-ice water and open water salinity and temperature.

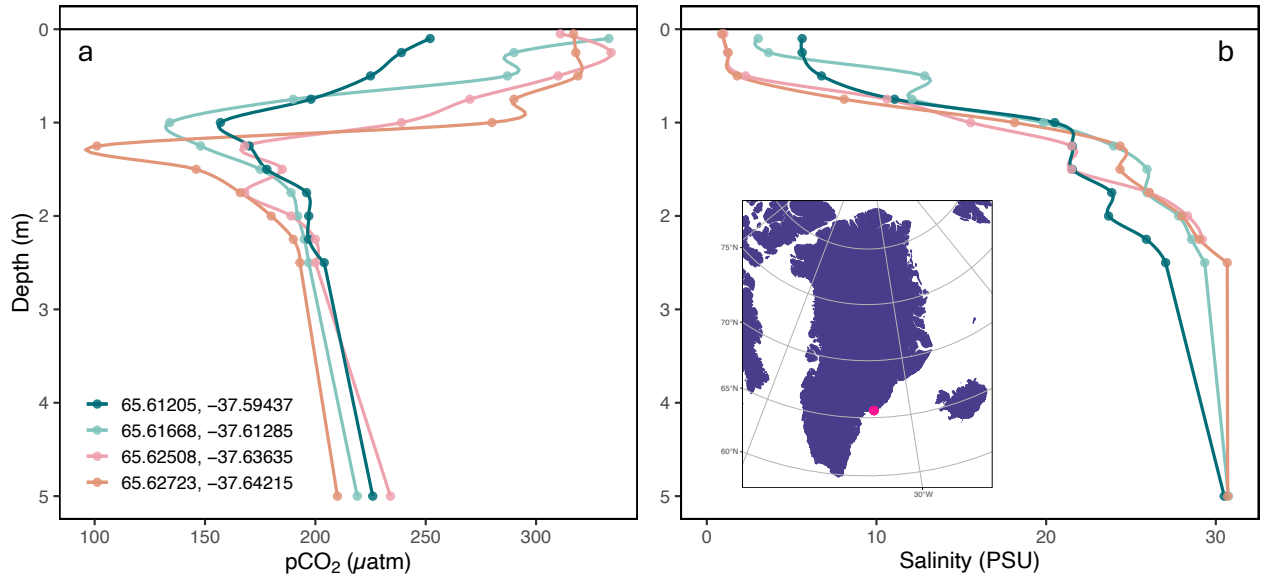

Figure 56. Measured pCO_2 (a) and salinity (b) profiles at 4 locations in Tasiilaq Bay. Profiles were measured on June 4, 2025 during the period of sea ice breakup following the method in Sejr et al. (2011).

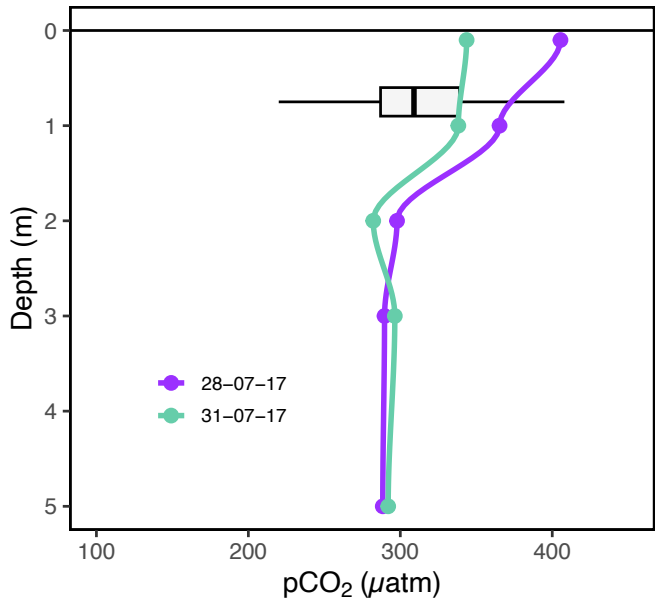

Figure 6~~7~~. Measured Young Sound pCO_2 profile after ice break up in 2017 compared with historical variation in pCO_2 at 1 m depth in the same location.

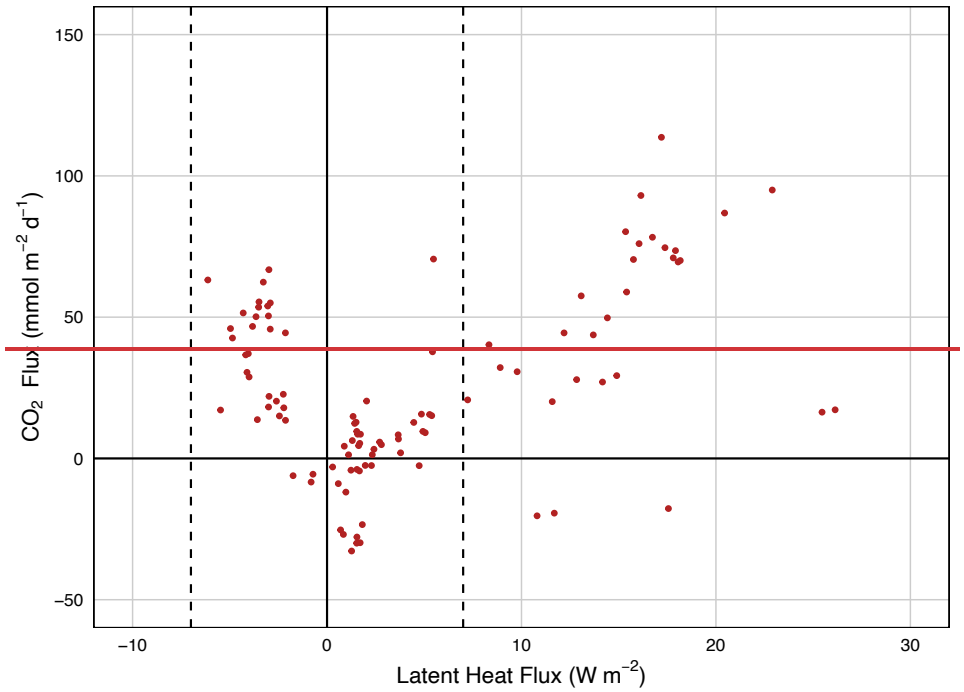

~~**Figure 8.** Relationship between CO_2 and latent heat fluxes measured using eddy covariance. Vertical dotted lines delineate the threshold (|LE| < ~7 W m^{-2}) where Landwehr et al. (2014) found negligible water vapor-related biases in measurements from the un-dried infrared gas analyzer. Data within this range demonstrate both CO_2 uptake and effluxes, indicating that air-sea CO_2 exchange may change direction during the dynamic period of sea ice melt.~~

4. Discussion

Air-sea CO_2 fluxes in Arctic coastal areas are generally estimated using bulk parameterization models (Henson et al., 2024; Meire et al., 2015; Roobaert et al., 2019; Sejr et al., 2011). These models rely on several key assumptions, including unstratified surface conditions, a linear pCO_2 gradient within the diffusive boundary layer, and a vertically uniform pCO_2 profile within the mixed layer. Our observations challenge the applicability of these assumptions in Arctic coastal waters in several important ways. We observe distinct vertical heterogeneity in both physical and chemical parameters, which leads to distinct differences in flux estimates based on the depth of the measurements used.

4.1. ~~Evaluating the Constant pCO_2 Assumption~~Stratified conditions in the marine CO_2 system

Vertical pCO_2 profiles collected during July 2017 revealed pronounced non-linear behavior in the upper 3 to 5 meters of the water column (Fig. 34). This directly contradicts the assumption that the ΔpCO_2 accurately represents the difference between the atmosphere and the "well-mixed bulk fluid" below the diffusive layer (Wanninkhof et al., 2009). Under ice-covered conditions, the lowest pCO_2 values (~150 ppm) were consistently observed just beneath the sea ice, with concentrations increasing with depth and stabilizing around 5 m (Fig. 34a). During the ice breakup stage, a similar pattern emerged, although the minimum pCO_2 was higher (~250 ppm).

More recent measurements from Tasiilaq Bay in June 2025 demonstrate very similar vertical pCO_2 profiles. Indeed, 4 high-resolution profiles with measurements every 0.25 m reveal the same C-shaped pCO_2 variation. Like in Young Sound, the most elevated pCO_2 levels were observed near the surface, and pCO_2 minimums occurred near 1-2 meters depth before increasing and becoming stable. This repeated observation in a different fjord system, but during the period of sea ice breakup indicates this vertical variability may be representative during stratified Arctic conditions.

Several interacting processes influence surface water chemistry during ice breakup. Low surface water pCO_2 values reflect the influence of low-salinity meltwater from snow and sea ice or glacial meltwater found in freshened Arctic waters (Geilfus et al., 2015; Henson et al., 2025). However, surface water chemistry during the ice breakup period is further complicated by processes such as ikaite ($CaCO_3 \cdot 6H_2O$) dissolution (Miller et al., 2011; Rysgaard et al., 2013; Søgaard et al., 2013) and high under-ice primary production (Søgaard et al., 2021). Additionally, snowmelt, characterized by low pH and ionic strength (de Caritat et al., 2005), may further alter carbonate system dynamics in the upper water column.

Two mechanisms may explain the nonlinear C-shaped trend in pCO_2 observed in the top few meters. First, as demonstrated by Henson et al. (2025) mixing between glacial meltwater and

seawater can result in nonlinear behavior in pCO_2, even when DIC and TA mix conservatively. In such cases, initial freshwater dilution leads to dramatically reduced pCO_2, but at very low salinities, the diminished buffering capacity can cause acidification to occur and pCO_2 to increase again. In fact, Henson et al. (2025) present a U-shaped pCO_2 curve along a salinity gradient that appears extraordinarily similar to the C-shaped pCO_2 curve we observe with depth. Indeed, the salinity gradient created in their mixing experiments can be observed vertically in the highly stratified surface waters during sea ice breakup (Fig. 3a, 5a). Although, Henson et al. focused on the influence of glacial meltwater, our results suggest similar processes could occur in systems influenced by sea ice and snowmelt.

Both glacial meltwater and sea ice have low DIC concentrations and act to dilute the inorganic carbon of the surface ocean (Fig. S4). However, changes in alkalinity can also impact the buffering capacity of the water mixture, leading to nonlinear effects. If the meltwater has a lower TA:DIC ratio than seawater, due to the absence of ikaite, acidification and a shift in carbonate equilibria at very low salinities could lead to higher pCO_2 values at the surface. During July 2017, Young Sound showed both diluted DIC and TA levels in upper few meters, suggesting pH change during sea ice break up could occur more easily (Fig. S4). Indeed, calculated pH profiles indicated variable surface conditions between periods of sea ice cover and sea ice breakup (Fig. S5). In this very fresh surface layer, diminished pH may elevate pCO_2 relative to waters around 1 m depth, where freshwater-seawater mixing ratios are more moderate and seawater buffering leads to very low CO_2 concentrations.

A second, but less likely, explanation involves atmospheric equilibration of sea ice melt ponds before draining into open leads. The relatively elevated pCO_2 observed at ~0.1 m depth could reflect such partial equilibration. While chamber-based studies (e.g. Geilfus et al., 2012, 2015; Nomura et al., 2010; Semiletov et al., 2004) have demonstrated both uptake and efflux of CO_2 in melt ponds, equilibrium times between melt-pond water and atmosphere depend upon pond depth, wind speed, and carbonate chemistry. For example, a 0.1 m deep pond under low wind conditions (~2 m s^{-1}) may reach atmospheric equilibrium in 1-4 days. However, in our case, pCO_2 values calculated from TA and DIC in melt ponds did not indicate equilibrium with the atmosphere, making this explanation less likely than the freshwater mixing mechanism. Nevertheless, atmospheric equilibration may play a role after the sea ice barrier is removed. Elevated pCO_2 levels at the surface (0.1 m) post sea ice breakup may result from the combination of the chemical changes described above, heating from solar radiation, and from atmospheric CO_2 uptake (partial equilibration) in the limited volume of this freshwater lens.

As melt progresses and sea ice recedes, riverine input and vertical mixing become more influential. Yet even after ice breakup, surface waters often remain fresh due to glacial meltwater runoff, and the resulting low salinities help maintain stratification. In August 2017, vertical structure remained pronounced even after sea ice breakup, with elevated pCO_2 at 0.1 m which

stabilized below ~3 m. In other words, near-surface conditions remained decoupled from deeper waters. This persistent shallow layer, characterized by low salinity, higher temperature, and elevated pCO_2, suppresses gas exchange with the colder, more undersaturated water below, consistent with observations by Dong et al. (2021). In such environments, bulk flux models that assume homogeneity and linear gradients are likely to yield biased or inaccurate estimates.

To place these 2017 measurements in historical context, we examined long-term surface water pCO_2 data collected at 0.5-1 m depth by the Greenland Ecosystem Monitoring (GEM) program between 2007 and 2023. These data, measured using consistent protocols, are presented in Fig. 6~~7~~ alongside our open-water profiles. Over the 17-year record, August pCO_2 concentrations at ~1 m depth had ranged from 220 to 408 µatm and had consistently remained below atmospheric levels. This apparent stability has contributed to the perception of sustained CO_2 uptake throughout the summer season.

However, the high-resolution vertical profiles obtained during the 2017 field campaign ~~challenge~~ add nuance to this assumption. Elevated pCO_2 levels confined to the uppermost meter of the water column may go undetected in standard monitoring approaches that rely on fixed-depth sampling. These results suggest that the dynamic changes during sea ice melt can induce ~~short-lived~~ episodes of slowed uptake, air-sea equilibrium, or CO_2 outgassing ~~can occur during rapid environmental transitions such as sea ice breakup~~. Consequently, existing sampling protocols may underestimate surface variability and bias flux estimates, especially in stratified conditions where near-surface chemistry is decoupled from subsurface layers.

4.2. ~~Evaluating Bulk Model Flux Estimates~~Influence of surface stratification on fluxes

To assess ~~whether~~ how bulk models ~~are suitable for~~function when estimating CO_2 fluxes in an Arctic fjord influenced by sea ice and snow melt, we calculated fluxes using seawater pCO_2 measurements from multiple depths and two gas transfer velocity parameterizations. Specifically, we computed fluxes throughout July using pCO_2 measured at 0.1, 1, 2, and 4 m. To estimate the surface (interface) pCO_2 at 0 m, we adjusted the 1 m pCO_2 measurements to a derived skin temperature (Table 1), estimated from sensible heat fluxes (Fig. S6~~3b~~) ~~-~~following the parameterization of Smedman et al. (2007). Accounting for this skin layer correction is critical, as Woolf et al. (2016) demonstrated that neglecting the thermal skin and relying only on bulk sea surface temperature can introduce significant errors in flux estimates.

The resulting calculations (Table 1) show that estimated CO_2 fluxes vary significantly depending on the depth of the pCO_2 measurement. Notably, fluxes derived from 0.1 m differ markedly from those based on deeper values. Since many studies rely on pCO_2 measured at a fixed depth (often at 1 m or at a ship's seawater intake below 5 m), these results underscore the potential for misrepresentation of flux magnitude and direction ~~and magnitude~~ due to vertical heterogeneity in surface water chemistry.

~~Measured fluxes from eddy covariance (Fig. 3a) also exhibited large temporal variability. While micrometeorological methods integrate fluxes over a horizontal footprint, bulk flux models rely on single point pCO_2 gradients between air and water. Consequently, under heterogeneous or partially ice-covered conditions, the two methods are unlikely to yield identical results. However, a qualitative comparison between the two approaches remains informative. Notably, agreement between micrometeorological and bulk model estimates was only observed in late July, and only when in situ pCO_2 was normalized to the derived skin temperature. This aligns with the conclusions of Woolf et al. (2016) and Ford et al. (2024), who suggest that using skin-adjusted pCO_2 may improve flux estimates. Accurate application of this correction would require either direct measurements of skin temperature when sampling for the bulk method or high-resolution modeling of heat fluxes.~~

~~However, this agreement between methods did not hold before or immediately after ice breakup. During these periods, micrometeorological methods indicated episodes of large upward fluxes, while bulk model estimates suggested downward fluxes (-14 mmol m^{-2} d^{-1}). Although both methods yielded comparable magnitudes for downward fluxes, only the micrometeorological approach captured large upward events that could not be reconciled with surface water pCO_2 profiles alone.~~

Measurements from both Young Sound and Tasiilaq demonstrate that during sea ice breakup, pCO_2 levels are most elevated at the surface. This may be linked to acidification of the most freshened 0.5 m and a shift in the marine carbonate system, or partial equilibration due to air-sea gas transfer. If this acidified freshwater lens warms, for instance, due to solar radiation, pCO_2 may rise leading to oversaturation relative to atmospheric concentrations. Indeed, when pCO_2 measurements on July 31 were corrected for skin temperature, to estimate pCO_2 at the boundary layer, they suggested a transition from undersaturation to oversaturation (Table 1). While we did not directly observe this oversaturation in the vertical profiles, this likely reflects the inability to sample at the ~~very~~ sea surface ~~layer~~. ~~Moreover, profile measurements represent only single points in a system characterized by strong spatial and temporal variability during this seasonal transition.~~Nevertheless, the occurrence of stratification-related vertical ~~C-shaped~~ pCO_2 heterogeneity~~profiles during sea ice breakup~~, with levels most elevated at the surface, will slow air-sea gas transfer compared to when conditions are well mixed. Meanwhile, warming or acidification of the thin surface layer may periodically induce a ~~may help explain the apparent~~ reversal of flux direction~~-~~, as seen in some micrometeorological studies in Arctic coastal environments during sea ice breakup (e.g. Butterworth et al., 2025)~~. suggested by the micrometeorological approach.~~

~~Another potential explanation for the elevated CO_2 efflux that cannot be discounted involves cross-sensitivity between water vapor and CO_2 in open-path NDIR sensors (Blomquist et al.,~~

~~2014; Landwehr et al., 2014). Although the OGM processing method is designed to minimize humidity-induced artifacts and large-scale turbulent motions, it cannot entirely remove them. While many of the extreme eddy covariance measurements from Young Sound are likely influenced by humidity-CO_2 cross sensitivity, several lines of evidence indicate that some positive CO_2 fluxes may not solely be attributed to this artifact.~~

~~In their comparative methodological study, Landwehr et al. (2014) identified large biases in open-path NDIR sensors related to water-vapor fluctuations, but reported agreement between sensors operating with dried and undried air streams during periods of low latent heat flux ($|LE| \leq 7$ W m^{-2}), where humidity-related bias was negligible. When examining the subset of Young Sound data below this threshold, eddy covariance measurements exhibit both positive and negative CO_2 flux estimates (Fig. 8). Additionally, elevated CO_2 concentrations occur across a wide range of relative humidities (Fig. S6) Taken together, these patterns support the interpretation that some of the measured effluxes may represent real air-sea CO_2 exchange rather than solely resulting from cross-sensitivity artifacts. However, definitive quantification using this experimental setup remains impossible and future studies using closed-path sensors during Arctic seasonal transitions are required to robustly constrain the magnitude of CO_2 outgassing and uptake.~~

Overall, these findings echo those of Miller et al. (2019), who reported pronounced spatial heterogeneity in Arctic coastal pCO_2 and large differences in estimated fluxes depending on the sampling depth. The broader implications of this heterogeneity for seasonal or regional flux estimates remain unclear. However, if fluxes are upscaled from sparse, single-point measurements (e.g., once per month, as in Laruelle et al., 2014), substantial errors may result due to unrecognized spatial and temporal variability. Thus, our results emphasize the need for continuous, high-resolution observations of air-sea CO_2 fluxes, particularly in Arctic coastal systems affected by stratification and meltwater input. These observations will be essential for refining flux parameterizations, reducing uncertainty in carbon budget estimates, and improving the representation of Arctic shelf systems in global carbon models.

Table 1. CO_2 fluxes calculated based on pCO_2 measured at the different depth. The fluxes are calculated using the bulk model of Ho et al., 2006 and Nightingale et al. (2000). We have used locally measured wind speeds for the calculations to match flux measurements captured by eddy covariance.

						Ho (2006)	Nightingale (2000)
Date	Depth (m)	Temperature (°C)	Salinity (psu)	pCO_2 (µatm)	Wind Speed (m s^{-1})	Flux (mmol CO_2 m^{-2} day^{-1})	Flux (mmol CO_2 m^{-2} day^{-1})
16-Jul	0.0	3.0†	23	252‡	6.8	-14.88	-13.69
16-Jul	0.1	3.0	23	244	6.8	-15.78	-14.52
16-Jul	1.0	1.8	26	240	6.8	-16.12	-14.83
16-Jul	2.0	1.1	28	241	6.8	-15.93	-14.66
16-Jul	4.0	0.3	29	275	6.8	-12.19	-11.21
18-Jul	0.0	6.0†	7	262‡	3.3	-3.45	-3.38
18-Jul	0.1	4.3	7	244	3.3	-3.98	-3.90
18-Jul	1.0	3.2	14	233	3.3	-4.20	-4.11
18-Jul	2.0	2.3	21	278	3.3	-2.86	-2.79
18-Jul	4.0	0.6	29	295	3.3	-2.34	-2.29
28-Jul	0.0	10.0†	15	415‡	2.5	0.53	0.54
28-Jul	0.1	10.0	15	405	2.5	0.38	0.38
28-Jul	1.0	7.0	21	365	2.5	-0.22	-0.23
28-Jul	2.0	5.0	27	282	2.5	-1.43	-1.45
28-Jul	4.0	2.0	30	290	2.5	-1.32	-1.34
31-Jul	0.0	12.0†	15	401‡	2.0	0.20	0.21
31-Jul	0.1	10.0	15	343	2.0	-0.36	-0.38
31-Jul	1.0	8.0	21	338	2.0	-0.40	-0.42
31-Jul	2.0	5.0	27	282	2.0	-0.92	-0.97
31-Jul	4.0	2.0	30	294	2.0	-0.81	-0.85

† Denotes skin temperatures derived from heat fluxes. ‡Denotes pCO_2 values estimated from measurements at 1 m depth and adjusted to derived skin temperatures.

5 Conclusions

During the summer thaw, carbon chemistry and pCO_2 dynamics in Arctic coastal surface waters are significantly altered by the combined effects of snow and sea ice melt, terrestrial runoff, and biological activity. These influences lead to substantial variability in surface temperature, pH, dissolved inorganic carbon (DIC), and total alkalinity (TA), ultimately disrupting carbonate

system equilibrium in the upper water column. As a result, estimating air-sea CO_2 fluxes using traditional bulk models becomes highly uncertain during this period.

The sea ice breakup period, typically lasting 2-4 weeks, represents a particularly dynamic and complex phase in the annual cycle. Despite its brevity, this phase may have a disproportionate influence on total summer CO_2 uptake, given that open-water conditions in high Arctic fjords are limited to only 80-120 days per year (Sejr et al., 2011).

~~Improved flux estimates will require more detailed and spatially resolved investigations aimed at developing and validating gas exchange parameterizations tailored to the highly stratified and ice-affected conditions of Arctic fjords. In particular, new approaches are needed to estimate gas transfer velocities over waters influenced by snow and sea ice melt.~~ Air-sea gas e~~E~~xchange rates depend not only on the pCO_2 gradient between the atmosphere and surface water, but also on rapid, nonlinear changes in surface water chemistry driven by the composition and volume of meltwater and runoff.

~~Once more suitable parameterizations for gas transfer velocity are established, a~~Accurate flux estimation will ~~also~~ therefore require knowledge of the depth at which surface water pCO_2 becomes vertically homogeneous, combined with gas exchange parameterizations tailored to highly stratified and ice-affected conditions. Profiling pCO_2 in the upper water column is therefore essential to identify this depth and to constrain surface flux estimates reliably.

Several eddy covariance studies in other arctic environments report variable uptake and efflux of CO_2 during the sea ice breakup period (e.g. Butterworth et al., 2025). Building on these findings, our data provides the first step in understanding potential drivers behind this variability.~~Similarly, eddy covariance measurements in Young Sound exhibited both positive and negative CO_2 flux estimates during this seasonal transition. However, these upward fluxes were not captured by the bulk model.~~ Though, proper quantification of the mechanisms driving nonlinear pCO_2 profiles and the resulting uncertainty of flux estimates will require observations~~These variable and sometimes conflicting datasets~~ spanning the air-sea boundary. The current lack of these datasets underscores the need for studies that integrate continuous, direct CO_2 flux measurements with detailed observations of surface water carbonate chemistry, atmospheric forcing, skin temperature, and turbulence at the air-ice-water interface.

Such integrated measurements are critical to improving our understanding of the ~~frequency,~~ drivers~~,~~ and net effect of ~~episodic upward~~ sea ice melt-driven changes on CO_2 fluxes in Arctic coastal systems. Ultimately, this knowledge is essential to accurately quantify the seasonal and regional uptake of atmospheric CO_2 in the rapidly changing Arctic.

Acknowledgments

This study is a contribution to the GreenFeedback project (Greenhouse gas fluxes and earth system feedbacks, Grant agreement: 101056921), funded by the European Union under the Horizon Europe program, who also supported L.L.S and H.C.H's involvement. H.C.H. was additionally funded by the AUFF (Aarhus Universitets Forskningsfond, project no. AUFF-F-2021-7-7) as part of his PhD. S.R. was funded by Aage V Jensens Fonde (grant no. AVJF21-3012) and the Danish National Research Foundation (grant no. DNRF 185). MKS was funded by the POMP project (Horizon Europe grant: 101136875) and the Connecting the Dots project (Villum Foundation grant: 50110) D.H.S received financial support from the Greenland Climate Research Centre (GCRC), Greenland Institute of Natural Resources. The study also received financial support from The Danish Ministry of Climate, Energy and Utilities, Programme for Arctic Climate, (project: Drivhusgas-observationer i Arktis (ObsArktis), 2017). Furthermore we received support from The Arctic Research Centre, Aarhus University and Greenland Institute of Natural Science. The authors especially wish to thank Egon Randa Frandsen, who assisted with the logistics and the additional measurements in Young Sound. Additionally, the authors would like to recognize the students in the EnCHil Nordic master program, who participated in taking the Tasiilaq measurements. This work is a contribution to the Arctic Science Partnership (ASP) and the MarinBasis component of the Greenland Ecosystem Monitoring Program.

Author Contribution

Conceptualization: LLS. Formal analysis, writing – original draft preparation: HCH. Funding acquisition: LLS, SR, MKS, TP. Investigation: DS, BJ, KL, TP, MKS, JS, SR, LLS. Writing – review and editing: DS, TP, MKS, SR, LLS. All the authors have read and agreed to the published version of the paper.

Data Availability Statement

Vertical profiles from both Greenlandic fjords can be found in the Zenodo data repository: https://doi.org/10.5281/zenodo.17471918

Competing interests

The authors declare no competing interests.

References

Ahmed, M. M. M., Else, B. G. T., Capelle, D., Miller, L. A., and Papakyriakou, T.: Underestimation of surface *p* CO2 and air-sea CO2 fluxes due to freshwater stratification in an Arctic shelf sea, Hudson Bay, Elementa: Science of the Anthropocene, 8, 084, https://doi.org/10.1525/elementa.084, 2020.

Arrigo, K. R. and van Dijken, G. L.: Continued increases in Arctic Ocean primary production, Progress in Oceanography, 136, 60–70, https://doi.org/10.1016/j.pocean.2015.05.002, 2015.

Bates, N. R. and Mathis, J. T.: The Arctic Ocean marine carbon cycle: evaluation of air-sea CO2 exchanges, ocean acidification impacts and potential feedbacks, Biogeosciences, 6, 2433–2459, 2009.

Burgers, T. M., Miller, L. A., Thomas, H., Else, B. G. T., Gosselin, M., and Papakyriakou, T.: Surface Water CO2 Variations and Sea-Air CO2 Fluxes During Summer in the Eastern Canadian Arctic, J. Geophys. Res. Oceans, 122, 9663–9678, https://doi.org/10.1002/2017jc013250, 2017.

Butterworth, B. J., Else, B. G. T., Brown, K. A., Mundy, C. J., Williams, W. J., Rotermund, L. M., and de Boer, G.: Annual carbon dioxide flux over seasonal sea ice in the Canadian Arctic, EGUsphere, 1–30, https://doi.org/10.5194/egusphere-2025-1802, 2025.

de Caritat, P., Hall, G., Gìslason, S., Belsey, W., Braun, M., Goloubeva, N. I., Olsen, H. K., Scheie, J. O., and Vaive, J. E.: Chemical composition of arctic snow: concentration levels and regional distribution of major elements, Science of The Total Environment, 336, 183–199, https://doi.org/10.1016/j.scitotenv.2004.05.031, 2005.

Dai, M., Su, J., Zhao, Y., Hofmann, E. E., Cao, Z., Cai, W.-J., Gan, J., Lacroix, F., Laruelle, G. G., Meng, F., Müller, J. D., Regnier, P. A. G., Wang, G., and Wang, Z.: Carbon Fluxes in the Coastal Ocean: Synthesis, Boundary Processes, and Future Trends, Annu. Rev. Earth Planet. Sci., 50, 593–626, https://doi.org/10.1146/annurev-earth-032320-090746, 2022.

Dong, Y., Yang, M., Bakker, D. C. E., Liss, P. S., Kitidis, V., Brown, I., Chierici, M., Fransson, A., and Bell, T. G.: Near-Surface Stratification Due to Ice Melt Biases Arctic Air-Sea CO $_2$ Flux Estimates, Geophysical Research Letters, 48, https://doi.org/10.1029/2021GL095266, 2021.

Garbe, C. S., Rutgersson, A., Boutin, J., de Leeuw, G., Delille, B., Fairall, C. W., Gruber, N., Hare, J., Ho, D. T., Johnson, M. T., Nightingale, P. D., Pettersson, H., Piskozub, J., Sahlée, E., Tsai, W., Ward, B., Woolf, D. K., and Zappa, C. J.: Transfer Across the Air-Sea Interface, in: Ocean-Atmosphere Interactions of Gases and Particles, edited by: Liss, P. S. and Johnson, M. T., Springer, Berlin, Heidelberg, 55–112, https://doi.org/10.1007/978-3-642-25643-1_2, 2014.

Gattuso, J.-P., Epitalon, J.-M., Lavigne, H., Orr, J., Gentili, B., Hagens, M., Hofmann, A., Mueller, J.-D., Proye, A., Rae, J., and Soetaert, K.: seacarb: Seawater Carbonate Chemistry, 2024.

Geilfus, N.-X., Carnat, G., Papakyriakou, T., Tison, J.-L., Else, B., Thomas, H., Shadwick, E., and Delille, B.: Dynamics of pCO2 and related air-ice CO2 fluxes in the Arctic coastal zone (Amundsen Gulf, Beaufort Sea), J. Geophys. Res., 117, n/a-n/a, https://doi.org/10.1029/2011JC007118, 2012.

Geilfus, N.-X., Galley, R. J., Crabeck, O., Papakyriakou, T., Landy, J., Tison, J.-L., and Rysgaard, S.: Inorganic carbon dynamics of melt-pond-covered first-year sea ice in the Canadian Arctic, Biogeosciences, 12, 2047–2061, https://doi.org/10.5194/bg-12-2047-2015, 2015.

Granskog, M. A., Kuzyk, Z. Z. A., Azetsu-Scott, K., and Macdonald, R. W.: Distributions of runoff, sea-ice melt and brine using δ18O and salinity data — A new view on freshwater cycling in Hudson Bay, Journal of Marine Systems, 88, 362–374, https://doi.org/10.1016/j.jmarsys.2011.03.011, 2011.

Hansen, J. W., Thamdrup, B., and J□rgensen, B. B.: Anoxic incubation of sediment in gas-tight plastic bags: a method for biogeochemical process studies, Marine Ecology Progress Series, 208, 273–282, 2000.

Haraldsson, C., Anderson, L. G., Hassellöv, M., Hulth, S., and Olsson, K.: Rapid, high-precision potentiometric titration of alkalinity in ocean and sediment pore waters, Deep Sea Research Part I: Oceanographic Research Papers, 44, 2031–2044, https://doi.org/10.1016/S0967-0637(97)00088-5, 1997.

Henson, H. C., Holding, J. M., Meire, L., Rysgaard, S., Stedmon, C. A., Stuart-Lee, A., Bendtsen, J., and Sejr, M.: Coastal freshening drives acidification state in Greenland fjords, Science of The Total Environment, 855, 158962, https://doi.org/10.1016/j.scitotenv.2022.158962, 2023.

687 Henson, H. C., Sejr, M., Meire, L., Sørensen, L. L., Winding, M. H. S., and Holding, J. M.: Resolving Heterogeneity
688 in CO2 Uptake Potential in the Greenland Coastal Ocean, Journal of Geophysical Research: Biogeosciences, 129,
689 e2024JG008246, https://doi.org/10.1029/2024JG008246, 2024.

690 Henson, H. C., Puts, I. C., Sejr, M. K., Sørensen, L. L., and Holding, J. M.: Glacial meltwater increases coastal
691 carbon dioxide uptake and sensitivity to biogeochemical change, Commun Earth Environ, 6, 687,
692 https://doi.org/10.1038/s43247-025-02685-4, 2025.

693 Jørgensen, H. E., Sørensen, L. L., and Larsen, S. E.: A Simple Model of Chemistry Effects on the Air-Sea CO2
694 Exchange Coefficient, Journal of Geophysical Research: Oceans, 125, e2018JC014808,
695 https://doi.org/10.1029/2018JC014808, 2020.

696 Laruelle, G. G., Lauerwald, R., Pfeil, B., and Regnier, P.: Regionalized global budget of the CO 2 exchange at the
697 air-water interface in continental shelf seas, Global Biogeochemical Cycles, 28, 1199–1214,
698 https://doi.org/10.1002/2014GB004832, 2014.

699 Liss, P. S. and Slater, P. G.: Flux of Gases across the Air-Sea Interface, Nature, 247, 181–184,
700 https://doi.org/10.1038/247181a0, 1974.

701 Lueker, T. J., Dickson, A. G., and Keeling, C. D.: Ocean pCO2 calculated from dissolved inorganic carbon,
702 alkalinity, and equations for K1 and K2: validation based on laboratory measurements of CO2 in gas and seawater at
703 equilibrium, Marine Chemistry, 70, 105–119, https://doi.org/10.1016/s0304-4203(00)00022-0, 2000.

704 Meire, L., Søgaard, D. H., Mortensen, J., Meysman, F. J. R., Soetaert, K., Arendt, K. E., Juul-Pedersen, T., Blicher,
705 M. E., and Rysgaard, S.: Glacial meltwater and primary production are drivers of strong
706 CO₂ uptake in fjord and coastal waters adjacent to the Greenland Ice Sheet,
707 Biogeosciences, 12, 2347–2363, https://doi.org/10.5194/bg-12-2347-2015, 2015.

708 Meire, L., Mortensen, J., Meire, P., Juul-Pedersen, T., Sejr, M. K., Rysgaard, S., Nygaard, R., Huybrechts, P., and
709 Meysman, F. J. R.: Marine-terminating glaciers sustain high productivity in Greenland fjords, Glob Change Biol, 23,
710 5344–5357, https://doi.org/10.1111/gcb.13801, 2017.

711 Miller, L. A., Papakyriakou, T. N., Collins, R. E., Deming, J. W., Ehn, J. K., Macdonald, R. W., Mucci, A., Owens,
712 O., Raudsepp, M., and Sutherland, N.: Carbon dynamics in sea ice: A winter flux time series, J. Geophys. Res., 116,
713 C02028, https://doi.org/10.1029/2009JC006058, 2011.

714 Miller, L. A., Burgers, T. M., Burt, W. J., Granskog, M. A., and Papakyriakou, T. N.: Air-Sea CO 2 Flux Estimates
715 in Stratified Arctic Coastal Waters: How Wrong Can We Be?, Geophys. Res. Lett., 46, 235–243,
716 https://doi.org/10.1029/2018gl080099, 2019.

717 Nomura, D., Yoshikawa-Inoue, H., Toyota, T., and Shirasawa, K.: Effects of snow, snowmelting and refreezing
718 processes on air–sea-ice CO2 flux, Journal of Glaciology, 56, 262–270,
719 https://doi.org/10.3189/002214310791968548, 2010.

720 Perovich, D., Meier, W., Tschudi, M., Hendricks, S., Petty, A. A., Divine, D., Farrell, S., Gerland, S., Haas, C.,
721 Kaleschke, L., Pavlova, O., Ricker, R., Tian-Kunze, X., Webster, M., and Wood, K.: Arctic Report Card 2020: Sea
722 Ice, 2020.

723 Raimondi, L., Matthews, J. B. R., Atamanchuk, D., Azetsu-Scott, K., and Wallace, D. W. R.: The internal
724 consistency of the marine carbon dioxide system for high latitude shipboard and *in situ* monitoring, Marine
725 Chemistry, 213, 49–70, https://doi.org/10.1016/j.marchem.2019.03.001, 2019.

726 Roobaert, A., Laruelle, G. G., Landschützer, P., Gruber, N., Chou, L., and Regnier, P.: The Spatiotemporal
727 Dynamics of the Sources and Sinks of CO2 in the Global Coastal Ocean, Global Biogeochemical Cycles, 33, 1693–
728 1714, https://doi.org/10.1029/2019GB006239, 2019.

729 Rysgaard, S., Vang, T., Stjernholm, M., Rasmussen, B., Windelin, A., and Kiilsholm, S.: Physical Conditions,
730 Carbon Transport, and Climate Change Impacts in a Northeast Greenland Fjord, Arctic, Antarctic, and Alpine
731 Research, 35, 301–312, https://doi.org/10.1657/1523-0430(2003)035%255B0301:PCCTAC%255D2.0.CO;2, 2003.

732 Rysgaard, S., Søgaard, D. H., Cooper, M., Pućko, M., Lennert, K., Papakyriakou, T. N., Wang, F.,
733 Geilfus, N. X., Glud, R. N., Ehn, J., McGinnis, D. F., Attard, K., Sievers, J., Deming, J. W., and Barber, D.: Ikaite
734 crystal distribution in winter sea ice and implications for CO2 system dynamics, The Cryosphere, 7, 707–718,
735 https://doi.org/10.5194/tc-7-707-2013, 2013.

736 Sejr, Krause-Jensen, D., Rysgaard, S., Sørensen, L. L., Christensen, P. B., and Glud, R. N.: Air—sea flux of CO2 in
737 arctic coastal waters influenced by glacial melt water and sea ice, Tellus B: Chemical and Physical Meteorology, 63,
738 815–822, https://doi.org/10.1111/j.1600-0889.2011.00540.x, 2011.

739 Sejr, M. K., Stedmon, C. A., Bendtsen, J., Abermann, J., Juul-Pedersen, T., Mortensen, J., and Rysgaard, S.:
740 Evidence of local and regional freshening of Northeast Greenland coastal waters, Sci Rep, 7, 13183,
741 https://doi.org/10.1038/s41598-017-10610-9, 2017.

742 Semiletov, I., Makshtas, A., Akasofu, S., and L Andreas, E.: Atmospheric CO_2 balance: The role of Arctic sea ice,
743 Geophysical Research Letters, 31, 2003GL017996, https://doi.org/10.1029/2003GL017996, 2004.

744 Sievers, Papakyriakou, T., Larsen, S. E., Jammet, M. M., Rysgaard, S., Sejr, M., and Sørensen, L. L.: Estimating
745 surface fluxes using eddy covariance and numerical ogive optimization, Atmospheric Chemistry and Physics, 15,
746 2081–2103, https://doi.org/10.5194/acp-15-2081-2015, 2015a.

747 Sievers, J., Papakyriakou, T., Larsen, S. E., Jammet, M. M., Rysgaard, S., Sejr, M. K., and Sørensen, L. L.:
748 Estimating surface fluxes using eddy covariance and numerical ogive optimization, Atmospheric Chemistry and
749 Physics, 15, 2081–2103, https://doi.org/10.5194/acp-15-2081-2015, 2015b.

750 Smedman, A., Högström, U., Sahlée, E., and Cecilia, J.: Critical re-evaluation of the bulk transfer coefficient for
751 sensible heat over the ocean during unstable and neutral conditions, Quart J Royal Meteoro Soc, 133, 227–250,
752 https://doi.org/10.1002/qj.6, 2007.

753 Søgaard, D. H., Thomas, D. N., Rysgaard, S., Glud, R. N., Norman, L., Kaartokallio, H., Juul-Pedersen, T., and
754 Geilfus, N.-X.: The relative contributions of biological and abiotic processes to carbon dynamics in subarctic sea
755 ice, Polar Biol, 36, 1761–1777, https://doi.org/10.1007/s00300-013-1396-3, 2013.

756 Søgaard, D. H., Sorrell, B. K., Sejr, M. K., Andersen, P., Rysgaard, S., Hansen, P. J., Skyttä, A., Lemcke, S., and
757 Lund-Hansen, L. C.: An under-ice bloom of mixotrophic haptophytes in low nutrient and freshwater-influenced
758 Arctic waters, Sci Rep, 11, 2915, https://doi.org/10.1038/s41598-021-82413-y, 2021.

759 Sulpis, O., Lauvset, S. K., and Hagens, M.: Current estimates of K_1* and K_2* appear inconsistent with measured
760 CO_2 system parameters in cold oceanic regions, Ocean Science, 16, 847–862, https://doi.org/10.5194/os-16-847-
761 2020, 2020.

762 Wanninkhof, R., Asher, W., Ho, D., Sweeney, C., and McGillis, W.: Advances in Quantifying Air-Sea Gas
763 Exchange and Environmental Forcing*, Annual review of marine science, 1, 213–44,
764 https://doi.org/10.1146/annurev.marine.010908.163742, 2009.

765 Watts, J., Bell, T. G., Anderson, K., Butterworth, B. J., Miller, S., Else, B., and Shutler, J.: Impact of sea ice on air-
766 sea CO2 exchange – A critical review of polar eddy covariance studies, Progress in Oceanography, 201, 102741,
767 https://doi.org/10.1016/j.pocean.2022.102741, 2022.

768 Woolf, D. K., Land, P. E., Shutler, J. D., Goddijn-Murphy, L. M., and Donlon, C. J.: On the calculation of air-sea
769 fluxes of CO2 in the presence of temperature and salinity gradients, Journal of Geophysical Research: Oceans, 121,
770 1229–1248, https://doi.org/10.1002/2015JC011427, 2016.

771